The Satellite Population Around Luminous Red Galaxies in the Legacy Surveys

Mindy Townsend

B.A. Political Science, Pittsburg State University, 2007

J.D. Washurn University School of Law, 2010

B.S. Physics, Washburn University, 2016

Submitted to the graduate degree program in Department of Physics and Astronomy and the Graduate Faculty of the University of Kansas in partial fulfillment of the requirements for the degree of Master of Science.

Committee members

Gregory Rudnick, Chairperson

Allison Kirkpatrick

Hume Feldman

Member 4

Member 5

Member 6

Member 7

Date defended: Feb. 03, 2020

The Thesis Committee for Mindy Townsend certifies
that this is the approved version of the following thesis :

The Satellite Population Around Luminous Red Galaxies in the Legacy Surveys

Gregory Rudnick, Chairperson

Date approved: March 03, 2020

Abstract

Luminous Red Galaxies, or LRGs, were originally selected in the Sloan Digital Sky Survey as good tracers of large scale structure. Subsequent investigations showed them to be among the most massive galaxies in the Universe and dominated by uniformly old stellar populations. Despite being dominated by old stars, however, they have grown in stellar mass since z=1, implying that they grow predominantly via accretion of mostly passive satellites. This picture has not yet been tested because of the lack of deep imaging data sets that both covers a large enough area of the sky to contain substantial numbers of LRGs and also is deep enough to detect faint satellites. I will present our initial characterization the satellite galaxy population of LRGs out to z=0.65. To accomplish this I use the Legacy Surveys, which are comprised of grz imaging to 2-2.5 mag deeper than SDSS, over a larger footprint, and with better image quality. Specifically, I will present our first measurement of the number of satellite galaxies around LRGs and how this number depends on LRG properties.

Acknowledgements

I would like to thank my partner Chris for his unwavering support (and who I can't believe didn't talk me out of this), John Moustakas of Sienna College for providing galaxy masses, and my advisor Greg for always sharing the chocolate he keeps in his desk.

Contents

List of Figures

0.1 Introduction

The method by which large elliptical galaxies accumulate their mass is an open question in galaxy evolution. There is evidence to suggest that massive galaxies grow hierarchically, that is, they grow by merging with other galaxies. For example, in their study of the growth of massive galaxies, van Dokkum et al. (2010) found that massive galaxies doubled their size since z = 2. They stacked rest frame R-band images and characterized the stellar distribution of these galaxies and determined that massive galaxies have gradually been building up their mass in the outer regions over the past 10 Gyr while the mass in the center 5 kpc remains mostly constant, indicating that massive galaxies have grown via mergers.

However, the details of this mass build-up in massive galaxies is not well understood. For example, number of studies have found that the stellar mass held in red galaxies has increased since z ~ 1. Bell et al. (2004) present the rest-frame colors and luminosities of ~25,000 galaxies in $0.2 < z < 1.1$ from the 0.78 deg^2 COMBO-17 survey (Classifying Objects by Medium-Band Observations in 17 Filters). They found that the B-band luminosity density does not evolve significantly in this redshift range, implying that there has been a build-up of stellar mass in the non-star forming population by a factor of 2 since z ~ 1. Faber et al. (2007) came to a similar result in their study that compares the luminosity functions of red and blue galaxies out to z ~ 1 of the DEEP2 and COMBO-17 surveys. They also find a virtually constant B-band luminosity density for red galaxies since z ~ 1, while the luminosity density of blue galaxies falls by ~0.6 dex. In their analysis of B-band luminosity function in NOAO Deep Wide Field Survey Bootes field, Brown et al. (2007) found similar growth in the stellar mass contained in the red galaxy population from $0.2 < z < 1.0$. They find that, for ~L* galaxies, the B-band luminosity density increases from z = 0 to z = 1 and that this population has roughly doubled its stellar mass in the past 8 Gyr.

However, this is not the case for $\simeq$ 4L* galaxies in the Brown et al. (2007) sample. They find that those more massive galaxies only differ slightly from their model with no mergers and negligible star formation at $z < 1$. The mass of the most massive galaxies have only grown by 20 percent since z = 0.7. They argue that growth via mergers may be more significant for low mass

galaxies, implying that the importance of satellite accretion may be different for different stellar mass galaxies. In addition, De Propris et al. (2010) derived an upper limit for a dry merger rate in their measurement of the fraction of Luminous Red Galaxies (LRGs) from the 2dF-SDSS LRG and QSO (2SLAQ) redshift survey in dynamically close pairs in the redshift range $0.45 < z < 0.65$. They find that major dry mergers (a luminosity ratio 1:4 or higher) are unimportant to the mass build-up of the red sequence at $z < 0.7$. In their study of the stellar mass functions of of quiescent and star-forming galaxies from z = 0 to z = 1, Moustakas et al. (2013) find that the number density of ~ 10^{10} M$\odot$ quiescent galaxies increases by a factor of 2-3 since $z \approx 0.6$, but the number density of > 10^{11} M$\odot$ is approximately constant from $z \approx 1$. They model the expected growth of galaxies due to star formation and find that mergers are not a dominant channel for stellar mass build-up in galaxies at $z < 1$.

There are theoretical reasons to believe that massive ellipiticals are important in understand how galaxies evolve. Multiple studies have shown that galaxies can be split into two distict populations: red quiescent and blue star forming galaxies. Springel et al. (2005) use hydrodynamical simulations to study the color transformation induced by star formation and active galactic nuclei (AGN) in merger remnants of star-forming disks. They found that a post-merger starburst will not necessarily consume all of the gas in the resulting elliptical galaxy. They found that AGN feedback can produce merger remnants that redden to $u - r \simeq 2.2 - 2.3$ in 1-2 Gyr and can leave a gas-poor remnant. To achieve the observed bimodality of galaxy color, mergers and AGN are necessary.

In their paper on the formation and evolution of brightest cluster galaxies (BCGs), De Lucia & Blaizot (2007) select massive dark matter halos at z = 0 from the Millinnium Simulation and study how and when the stars that make up the central galaxies form. They use merger trees to track the progenitors of z = 0 central galaxies. They find that 50 percent of the stars found in BCGs were already formed by z ~ 5. In addition, in only 40 percent of the z = 0 BCGs was the last major merger (defined as a merger between two galaxies with at least a 3:1 mass ratio) before z = 1. That number rises to only 65 percent before z = 0.5. Even though the stars in these galaxies are old, BCGs are not assembled until relatively recently. De Lucia & Blaizot (2007) find that, of the

BCGs in their sample, only 10 percent were formed before z ~ 1, and half were assembled after z ~ 0.5. Old stellar populations coupled with the late assembly times of these galaxies indicate that the BCGs in their sample gained most of their mass through accretion of satellite galaxies.

Furthermore, it has been shown that the way galaxies evolve in inextricably linked with their environment. De Lucia et al. (2012) use publicly available merger trees that are obtained from applying semi-analytic techniques to the Millennium Simulation to study the environmental history of groups and cluster galaxies, using . They make two main findings. First, on average, surviving massive ($\log_{10}(M/M_{\odot}) > 11$) satellites at z = 0 fell into the main progenitor of the final cluster later than less massive satellites. Second, there is a correlation between the time a galaxy becomes a satellite and its distance from the final cluster center. These two findings illustrate what the authors call "history bias," an important part of the hierarchical framework of galaxy evolution. In this framework, small systems form first and get bigger and bigger through subsequent mergers of these small systems. The findings in De Lucia et al. (2012) indicate that where a galaxy resides today (or any epoch) depends heavily on that galaxy's history and that galaxies of different masses will have different environmental histories. Studying galaxies in bins of stellar mass is not enough to fully understand their evolution.

Both observations and simulations indicate merger events are responsible for the mass build up of massive ellipticals, but in what mass regime this is dominant is inconclusive. Observations have shown that, at constant number density, the stellar mass in red sequence galaxies has doubled in at least the last 10 Gyr (van Dokkum et al. (2010)), and simulations have been quite successful in replicating observed phenomena using the hierarchical framework. However, the picture of mass growth of elliptical galaxies via mergers has yet to be tested because of the dearth of data that can identify faint satellites while at the same time encompassing a large sample of giant ellipticals. However, this situation is changing with the arrival of the DESI Legacy Imaging Surveys (Legacy Surveys). While large surveys have revolutionized the field of galaxy evolution, there has not until recently been data sets that both cover a large enough area of the sky to contain a substantial number of luminous ellipticals and deep enough to detect faint satellites. Surveys like SDSS are

too shallow to see very faint objects around luminous galaxies, and surveys like the NOAO Deep Wide-Field Survey only cover a small fraction of the sky. Using data from the Legacy Surveys, we can probe two magnitudes deeper compared to SDSS.

Here, we use the Legacy Surveys to characterize the satellite population around SDSS-identified luminous red galaxies. Originally selected as good tracers of large scale structure (Eisenstein et al. 2001), subsequent investigations have shown them to be among the most massive galaxies in the universe, dominated by uniformly old stellar populations (Tojeiro et al. (2011)). Despite this, the stellar mass of LRGs has grown since z=1, implying that they grow mostly through the accretion of passive satellites (see Cool et al. (2008)). Multiple studies have also shown that the spectra of LRGs indicate that those galaxies have undergone passive fading (e.g. Cool et al. (2008); Banerji et al. (2010), but see also Tojeiro & Percival (2011) which finds that bright LRGs evolve consistent with passive evolution, but fainter LRGs deviate from that). Using the deeper imaging from the Legacy Survey can allow for the study of satellite galaxy properties, as well as the constraint on the importance of mergers in the formation of massie passive galaxies like LRGs.

This paper is structured as follows: Section 2 describes the data and sample selection, Section 3 describes our statistical background subtraction method, we describe our results in Section 4, with Section 5 reserved for conclusions.

0.2 Data

0.2.1 The Legacy Surveys

The DESI Legacy Imaging Surveys are a trio of surveys that image $\approx$ 14,000 deg^2 of the extragalactic sky visible from the northern hemisphere in three optical bands - g, r, and z - with a combined survey footprint that is split into two contiguous regions by the galactic plane (Dey et al. 2018). Those surveys are the Dark Energy Camera Legacy Survey, the Beijing-Arizona Sky Survey, and the Mayall z-band Legacy Survey.

The Dark Energy Camera Legacy Survey (DECaLS) utilizes the Blanco 4-m telescope at Cerro

Tololo Inter-American Observatory using the Dark Energy Camera and covers 9,000 deg^2 combined of the Northern and Southern Galactic Cap. The survey obtains optical imaging data in the g-, r-, and z-bands and overlaps existing spectroscopy from the Sloan Digital Sky Survey (SDSS) and reaches depths of 24.0, 23.4, and 22.5 in the g-, r-, and z-band, respectively, more than two magnitudes deeper than SDSS. The Beijing-Arizona Sky Survey (BASS) utilizes the 90prime camera on the 2.3-m Bok Telescope at Kitt Peak National Observatory and covers 5,000 deg^2 of the Northern Galactic Cap. The survey obtains optical imaging data from the SDSS g- and r-bands and reaches depths of 24.0 and 23.6 in the g- and r-bands, respectively. The final survey, the Mayall z-band Legacy Survey (MzLS), only takes data in the z-band and utilizes the MOSAIC-3 camera at the prime focus of the 4-m Mayall Telescope at Kitt Peak. See Dey et al. (2018) for a more detailed explanation. Observed g-, r-, and z-band photometry is illustrated in 1. Source detection is performed using a forward modeling algorithm called The Tractor. This approach takes in individual images optical images, and for each source a model is fit simultaneously to pixel-level data. Each source is modeled using a set of parametric light profiles: a delta function, deVaucouleurs $r^{-1/4}$ law, exponential disk, or exponential disk plus deVaucouleurs. Each exposure is then convolved with each model to determine the best fit model. For this study we use the photometry from the 8th data release.

0.2.2 SDSS BOSS LRGs

The sample of LRGs were identified in the Baryon Oscillation Spectroscopic Survey (BOSS), part of the SDSS-III project. The BOSS LRGs are divided into a low redshift sample (LOWZ) and a constant-mass sample (CMASS) (Reid et al. 2016). Both the LOWZ and CMASS sample were selected based on a set of color- magnitude cuts. For the LOWZ sample, these cuts are designed to only select the brightest and reddest galaxies at low redshift ($z < 4$) and are similar to the SDSS-I/II Cut-I Luminous Red Galaxies. The LOWZ sample is also approximately volume-limited over $0.2 < z < 0.4$ with a constant space density of $\sim 3 \times 10^{-4}$ $h^3 Mpc^{-3}$. The CMASS sample includes galaxies between $0.4 < z < 0.7$ with an approximately constant stellar mass limit over the redshift

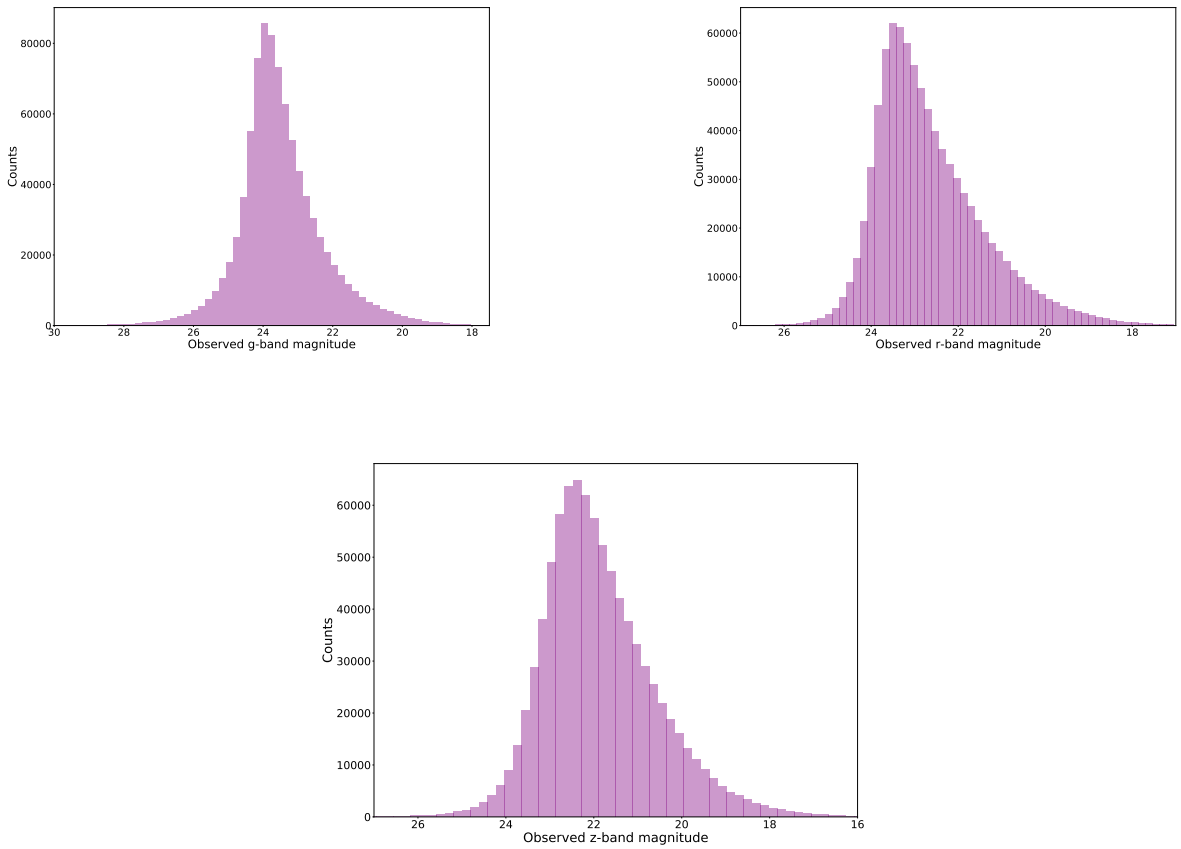

Figure 1: The observed g-, r-, and z-band magnitude distribution for Legacy Survey sources. The Legacy Surveys go about 2 magnitudes deeper than the SDSS depths of 22.2, 22.2, and 20.5 in the g-, r-, and z-bands, respectively.

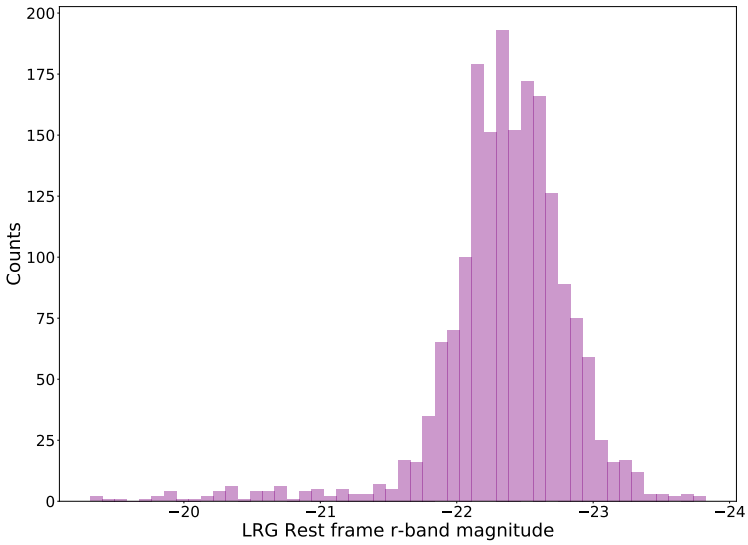

Figure 2: The absolute r-band magnitude distribution of the SDSS LOWZ and CMASS galaxy sample used in this paper. Absolute magnitudes are calculated according to Brammer et al. (2008). Luminous Red Galaxies occupy a relatively narrow range in absolute magnitudes.

range. The CMASS sample is also selected by a color cut, similar to SDSS-I/II Cut-II and 2SLAQ LRGs. However, the cuts are bluer and more faint to increase the number density of targets in the CMASS redshift range. Higher redshift galaxies in CMASS are isolated using (g-r) and (r-i) colors. Together, LOWZ and CMASS make a spectroscopic sample that is 80 percent complete at $\log_{10}(M/M_{\odot}) \geq 11.6$ at $z < 0.61$. For more details on the selection criteria for LOWZ and CMASS (see Reid et al. 2016).

I computed the rest frame magnitudes for BOSS LRGs using the photometric redshift code EAZY (Brammer et al. 2008). LRG stellar masses are computed using iSEDfit from Moustakas et al. (2013). iSEDfit uses Baysian inference to extract physical properties from a galaxy's observed broadband spectral energy distribution. For this study we use the photometry of the 8th data release of the Legacy Surveys and the spectroscopy from the 14th SDSS data release.

Figures 2, 3, and 4 show the rest frame magnitude, mass distrbutions, and redshift, respectively, of our sample of SDSS-identified LRGs.

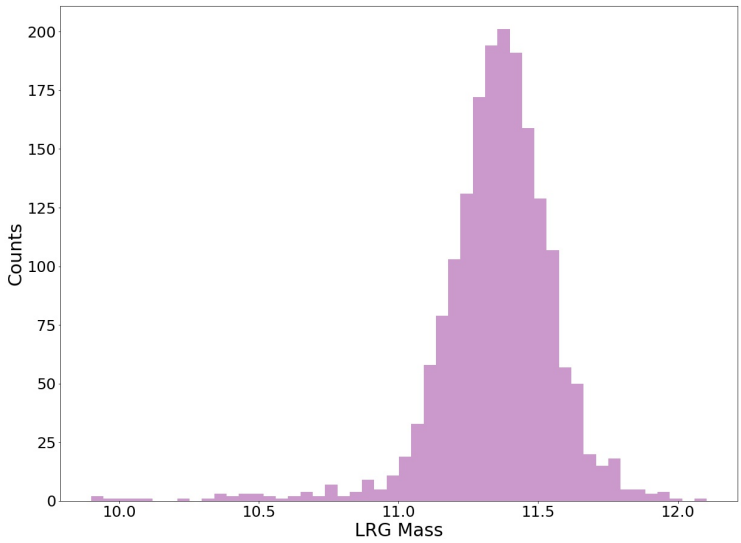

Figure 3: The mass distribution of the SDSS LOWZ and CMASS galaxy sample used in this paper. Masses are calculated according to Moustakas et al. (2013). Luminous Red Galaxies are some of the most massive galaxies in the universe and occupy a narrow range of masses.

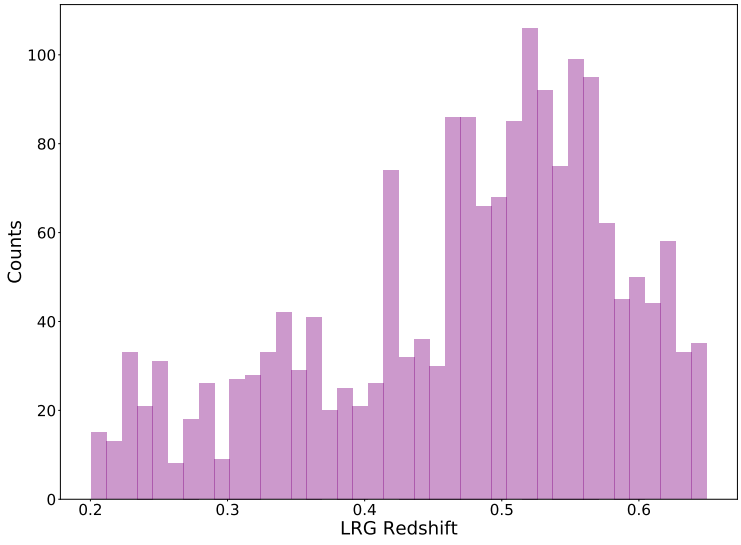

Figure 4: The redshift distribution of the SDSS LOWZ and CMASS galaxy sample used in this paper. The redshift range is from $0.2 < z < 0.65$. The median redshift of the LRG sample is $z \sim 0.5$.

0.2.3 Sample Selection

All galaxies in this study are subjected to a quality cut. Each image must have at least two images that contribute to the central pixel in each filter. Furthermore, we eliminated sources with a negative flux in the three observed bands, and the profiles of all sample galaxies are either classified as having a round exponential, de Vaucouleurs, or exponential profile. In addition, we set the first, fifth, sixth, seventh, eleventh, twelfth, and thirteenth bitmasks to zero so as to ensure that the sources are not compromised by bright stars, globular clusters, large galaxies, or bad pixels.

While 98 percent of the sources are observed at least twice (Dey et al. 2018), 74.33 percent and 23.8 percent of the survey had 3 and 4 exposure coverage, respectively. This results in non-uniform depths in our target area. To ensure constant depth over our target area, we have made a magnitude cut in the z-band. First we create a density map of galaxies in our field with HEALPix Gorski et al. (2005). HEALPix, or Hierarchical Equal Area isoLatitude Pixelisation, was first developed to allow for quick and accurate analysis of full-sky data sets like the Wilkinson Microwave Anisotropy Probe and Planck, but it works equally well to visualize the density of galaxies. HEALPix discretizes the surface of a sphere into equal-area, non-overlapping tiles called pixels. Astophysical analysis can be done on a per-pixel basis. We find and plot the distribution of the median z-band magnitude per pixel and excluded the faintest 10 percent of galaxies in our sample. Fig. 5 illustrates the effect on the density of the field. This results in the exclusion of Legacy Survey sources fainter than observed z-band magnitude 22.36. For the purposes of this study we limit our analysis to the Legacy Surveys Early Data Release (EDR), which includes 25 square degrees of the sky between 241 deg < RA < 246 deg and 6.5 deg < Dec < 11.5 deg. I use only the EDR as a convenience, as running the analysis on the entire overlapping Legacy Survey-SDSS footprint is too time-consuming. However, the EDR has a large enough sample size of LRGs that important information can still be found. There are 1823 LRGs that match the above criteria in the EDR.

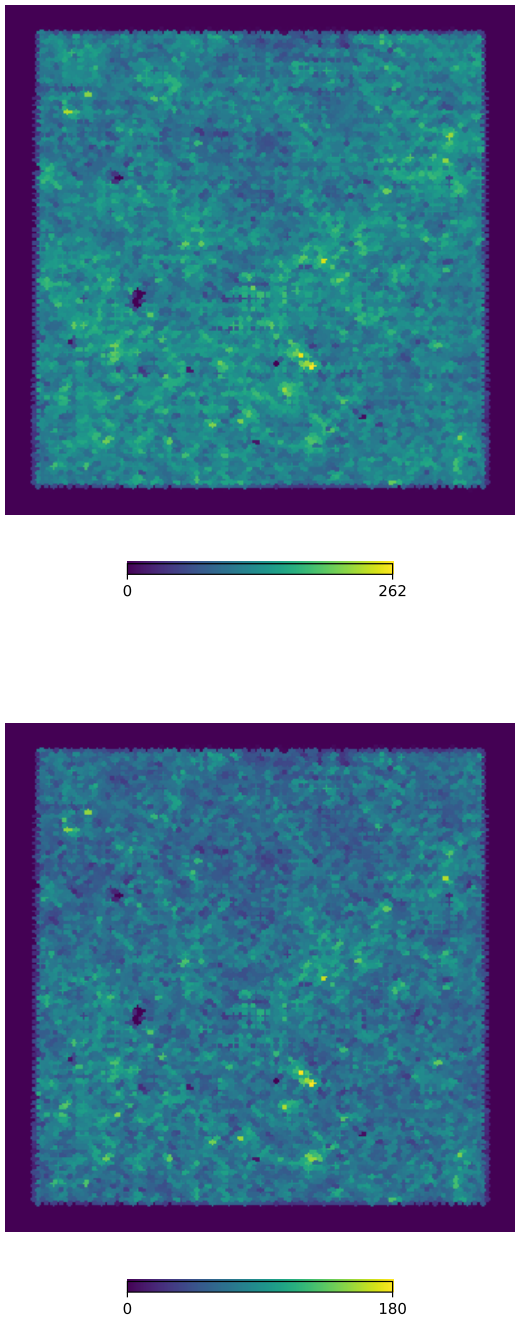

Figure 5: A density map of galaxies in the Legacy Survey Early Data Release, which includes 25 square degrees of the sky between 241 deg < RA < 246 deg and 6.5 deg < Dec < 11.5 deg. Circular gaps are masked bright stars. The color bar represents the number of sources in each pixel. Top: Density map of galaxies in the Legacy Survey before observed z-band magnitude cut. Bottom: Density map of galaxies in the Legacy Survey after observed z-band magnitude cut. I make a cut in the z-band magnitude to help ensure that overdense areas are likely large-scale structure and not the product of unequal depth over the field.

0.2.4 Completeness

The observed cut in the z-band magnitude is not enough to ensure that I am not missing faint sources, so I need to determine down to what luminosity I can reliably measure satellites. To determine the luminosity rest-frame completeness of the Legacy Survey sample, we calculate the rest-frame z-band magnitude of galaxies in the UltraVISTA catalog (Muzzin et al. 2013) using the photometric redshift code EAZY (Brammer et al. 2008). The UltraVISTA catalog is desirable because it has reliable photometric redshifts and is reasonably deep. We are interested in determining the luminosity completeness at the high redshift end of our sample, so we plot the luminosity histogram for UltraVISTA in the range of $0.55 \leq z \leq 0.65$ and the luminosity histogram for this redshift range with an additional observed z-band magnitude limit in the Legacy Surveys, which are functionally luminosity functions. We then plot the ratio of the counts as a function of luminosity for all galaxies in the respective samples and for red and blue galaxies, separately. The ratio for all galaxies in the sample is shown in Fig. 7 and the ratio for red and blue galaxies are shown in Figures 9 and 11, respectively. Red and blue galaxies are classified by rest frame U-V color calculated using EAZY and shown in Fig. 6: (U-V) > 1.4 for red galaxies and (U-V) < 1.4 for blue galaxies. We take the more conservative luminosity cutoff $\log_{10}(L/L_{\odot}) \sim 10.5$.

0.3 Statistical Subtraction Method

In this paper we report the number of satellite galaxies LRGs can be expected to have as a function of LRG properties. However, even though we have SDSS redshifts for our sample of LRGs, getting the same information for the faint sources that surround those galaxies is observationally infeasible. This is why we choose to perform a statistical background subtraction.

To calculate the number of satellite galaxies that live around LRGs, I need to estimate the number of background galaxies in bins of color and magnitude. From there I can statistically estimate how many galaxies there are above the background. In that way, I can ascertain the

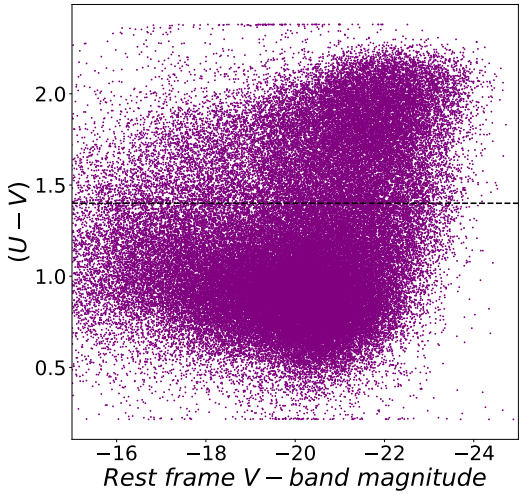

Figure 6: The color-magnitude diagram for all galaxies in the UltraVISTA catalog. Red and blue galaxies are classified by rest frame U-V color calculated using EAZY: (U-V) > 1.4 for red galaxies and (U-V) < 1.4 for blue galaxies. (U-V) = 1.4 is shown by the dashed line. The plot shows two clear galaxy populatios.

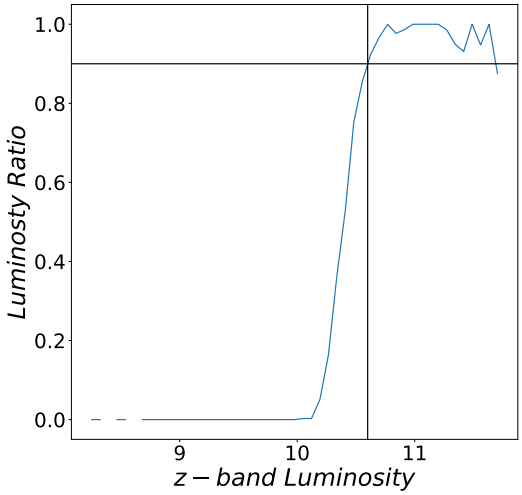

Figure 7: The ratio of luminosity histograms for UltraVISTA galaxies within 0.55 < z < 0.65 and brigher than the Legacy Survey observed z-band magnitude cut and all UltraVISTA galaxies in that redshift range. The horizontal line indicates 90 percent completeness and the vertical line indicates the corresponding rest frame z-band luminosity of 10.6.

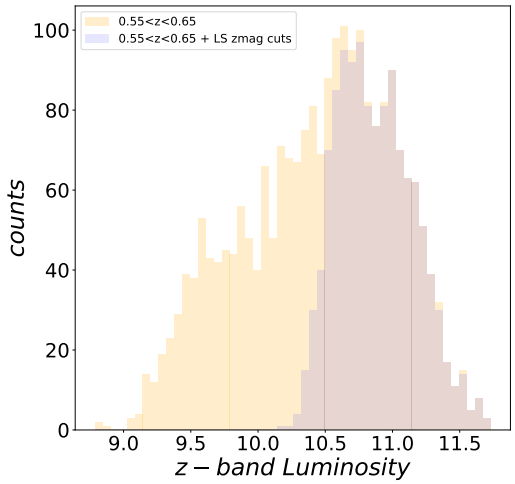

Figure 8: Histogram of red UltraVISTA galaxies in the redshift range 0.55 < z < 0.65 with observed z-band magnitude cut used for Legacy Survey sources overplotted over all red UltraVISTA sources in that redshift range. The histograms match at high luminosity but deviate at low luminosity, as expected with an observed magnitude cut.

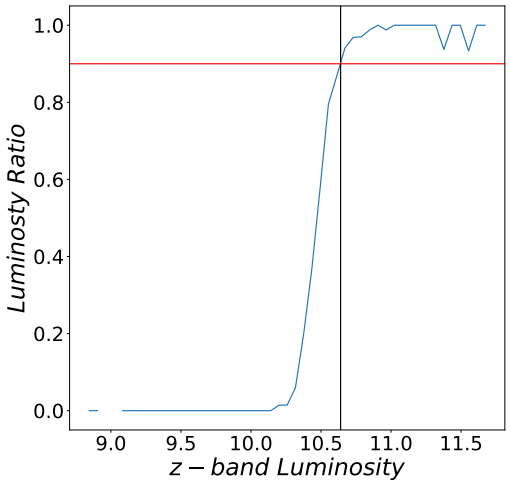

Figure 9: The ratio of luminosity histograms for red UltraVISTA galaxies within 0.55 < z < 0.65 and brigher than the Legacy Survey observed z-band magnitude cut and all UltraVISTA galaxies in that redshift range. The horizontal line indicates 90 percent completeness and the vertical line indicates the corresponding rest frame z-band luminosity of 10.6.

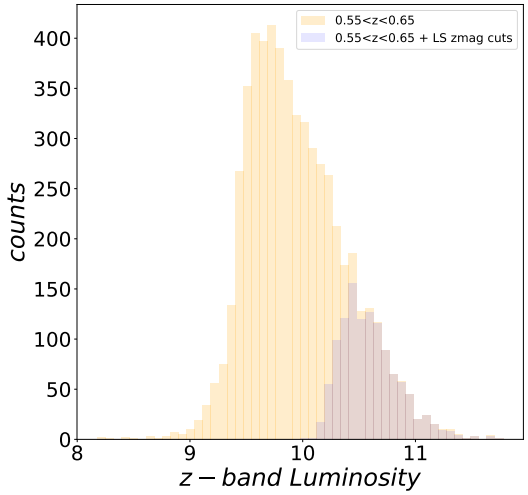

Figure 10: Histogram of blue UltraVISTA galaxies in the redshift range $0.55 < z < 0.65$ with observed z-band magnitude cut used for Legacy Survey sources overplotted over all blue UltraVISTA sources in that redshift range. The histograms match at high luminosity but deviate at lower luminosity, as expected with an observed magnitude cut.

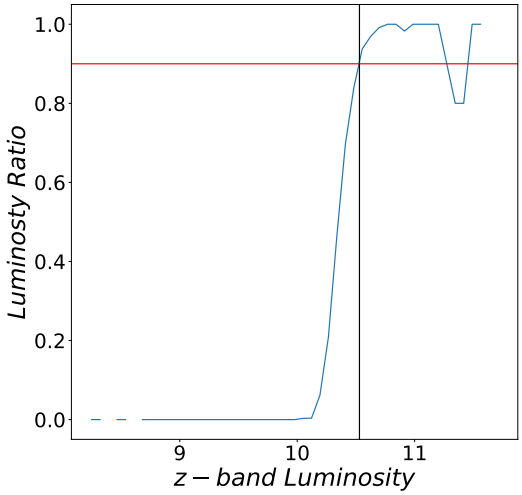

Figure 11: The ratio of luminosity histograms for blue UltraVISTA galaxies within $0.55 < z < 0.65$ and brigher than the Legacy Survey observed z-band magnitude cut and all UltraVISTA galaxies in that redshift range. The horizontal line indicates 90 percent completeness and the vertical line indicates the corresponding rest frame z-band luminosity of 10.5.

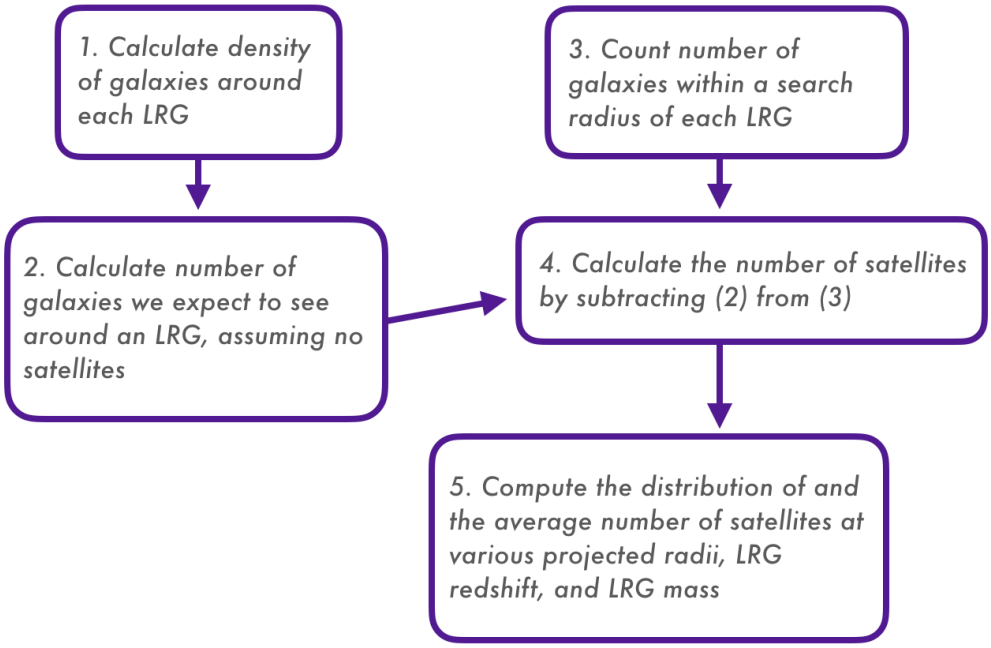

Figure 12: A summary schematic of my statistical background subtraction algorithm.

existence of a satellite population. The following is a brief description of the statistical background subtraction method used in this paper: First, we define a physical search radius in which we look for satellites. This radius is redshift-independent. Next, we count the number of near neighbors within a projected distance of the LRG using the k-d tree near neighbors function in scikit-learn (Varoquaux et al. 2015). Then, we calculate the local surface density around each LRG by counting the number of galaxies in an annulus with an inner radius of 0.4 degree and an outer radius of 0.5 degree from the LRG and dividing by the area of the annulus. The local surface density is calculated using HEALPix. This algorithm allows me to create an easily searchable map of Legacy Survey sources. This means I can calculate the background once for my entire field and quickly search for sources within a defined distance and calculate the area over which that search was conducted. An example of a HEALPix visualizaton can be found in Fig. 5. This inner distance for calculating the local surface density was chosen because, on average for our LRG sample, 0.4 degree is the distance at which large-scale structure starts to dominate the error. Fig. 13 shows the standard deviation (blue) and Poisson errors (red) of the measurement of the background for every LRG as a function of distance from the LRG in degree. The light blue and red lines are the median standard deviation and Poisson error, respectively. Poisson noise becomes subdominant at ~ 0.4 deg. Using this local surface density, we calculate the number of expected background galaxies by multiplying the local surface density by the redshift-dependent search radius. We then subtract the number of expected background galaxies from the number of projected near neighbors in bins of color and magnitude to find the number of expected satellite galaxies. Finally, each bin for each LRG is summed to get the number of satellite galaxies. A summary flowchart of this method is found in Fig. 12.

To ensure that our method does not return contributions from very different redshifts, we do the subtraction in bins of observed (r-z) color, (g-r) color, and z-band magnitude. We do this for two reasons. Galaxies at different redshifts can have similar observed (g-r) color, but very different observed (r-z) color. By doing the background subtraction in two colors, I can more accurately estimate the rest frame luminosity of each cell in the color-magnitude diagram. Using two colors

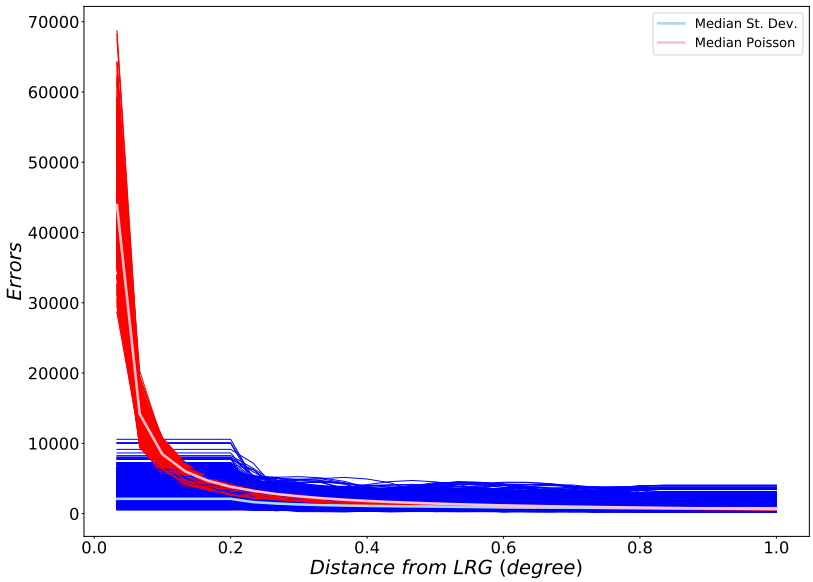

Figure 13: This plot shows the standard deviation (blue) and Poisson errors (red) of the measurement of the background for every LRG as a function of distance from the LRG in degree. The light blue and red lines are the median standard deviation and Poisson error, respectively. Poisson noise starts to be comparable to the standard deviation at ~ 0.4 deg, meaning that the large scale structure of the universe becomes the dominant source of error and we can assume that sources found at this distance are not physically associated with the LRG.

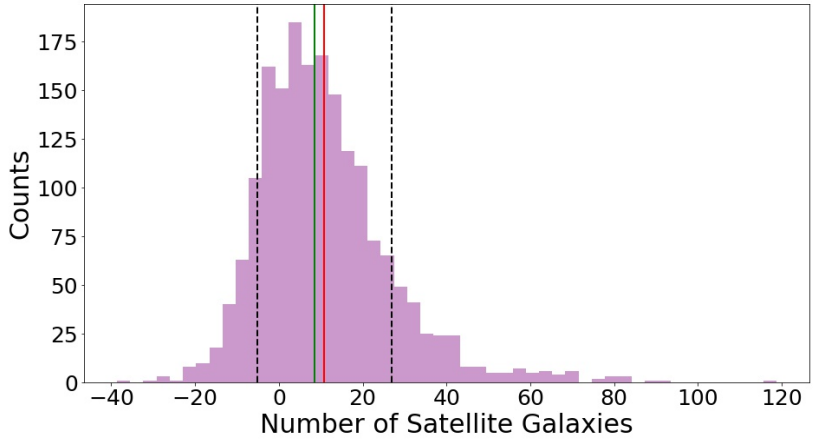

Figure 14: The distribution of the number of satellite galaxies calculated to be associated with SDSS-identified LRGs. The mean number of satellite galaxies for each LRG is $\sim$ 10.9. The red line marks the mean, the green line marks the median, and the dashed black lines are one standard deviation from the mean. The error in the mean is negligable.

allows us to constrain the rest frame luminosity of satellite galaxies that would not be possible using only (r-z) color or only (g-r) color. Doing the subtraction in two colors allows us to be more confident in the contribution to the rest frame luminosity of any particular color-color-magnitude cell.

0.4 Results

The main result of this paper is illustrated in the histogram of the number of satellite galaxies in Fig. 14. The red line is the mean, the green line is the median, and the black dashed line is one standard deviation from the mean. Measured over 1800 LRGs, the mean number of satellite galaxies is 10.9 and a median of 8.6. Some negative values are expected because of how the number of satellites are calculated. For each LRG, we subtract the number of "near neighbors" from the number of "interloper" galaxies. Random fluctuations in the measured background can cause negative values.

We can also see the breakdown the number of satellite galaxies by LRG redshift. As illustrated in Fig. 16, at lower redshift we on average see more satellite galaxies around LRGs when compared to LRGs at the high end of our redshift range. This is likely because faint satellites are easier to

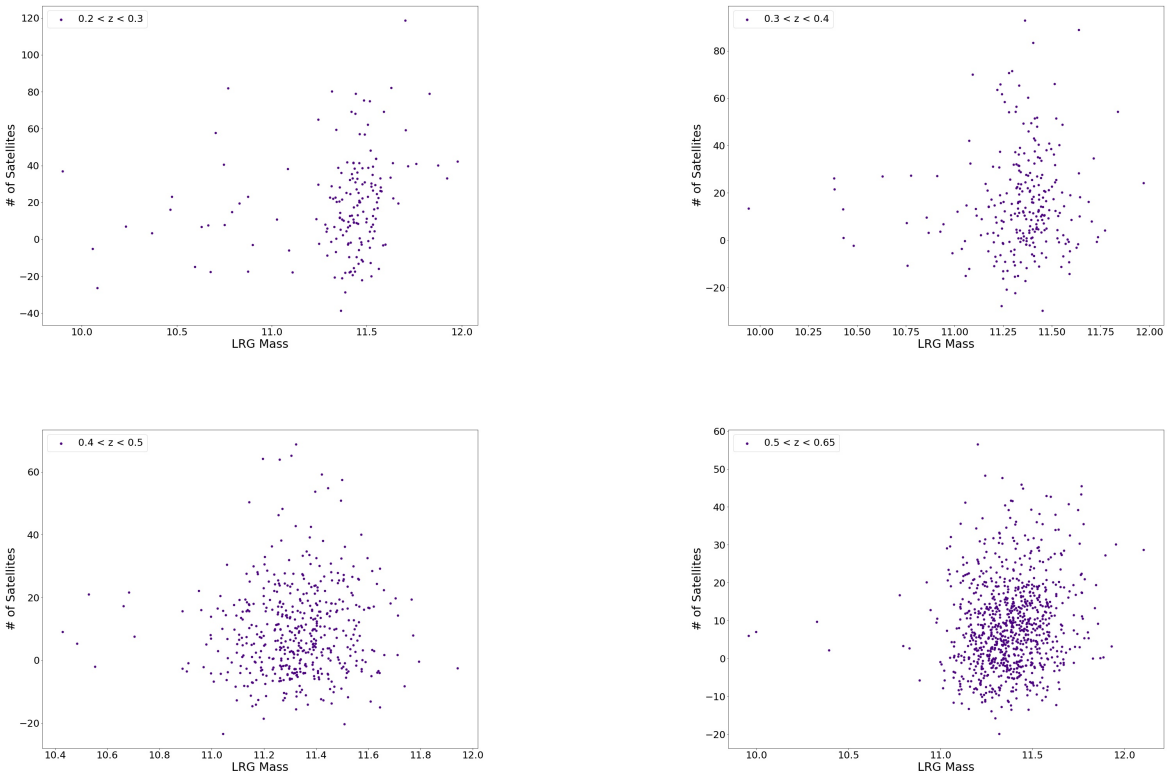

Figure 15: Number of satellites as a function of LRG mass in bins of redshift. Each point represents on LRG. While there is a large spread in the number of satellites, the number does not depend on LRG mass.

detect at low redshift. Fig. 15 indicates that there is little, if any, dependence of the number of satellites on LRG mass.

We can measure the observed color distribution of satellite galaxies and compare those colors to the colors of the LRGs. Figures 17a through 17d are color-magnitude diagrams for LRGs and satellite galaxies using (r-z) color and observed z-band magnitude in bins of redshift. The plot shows the color and magnitude of LRGs as dots overlaid on a density plot of satellite galaxies. Satellites are in general more faint in the observed z-band than their LRG hosts. This is unsurprising since Luminous Red Galaxies are known to be some of the biggest and brightest known galaxies. There are a population of satellites redder than the LRGs in observed (r-z) color, but in general the satellite population is around the same color or slightly bluer than the LRG hosts.

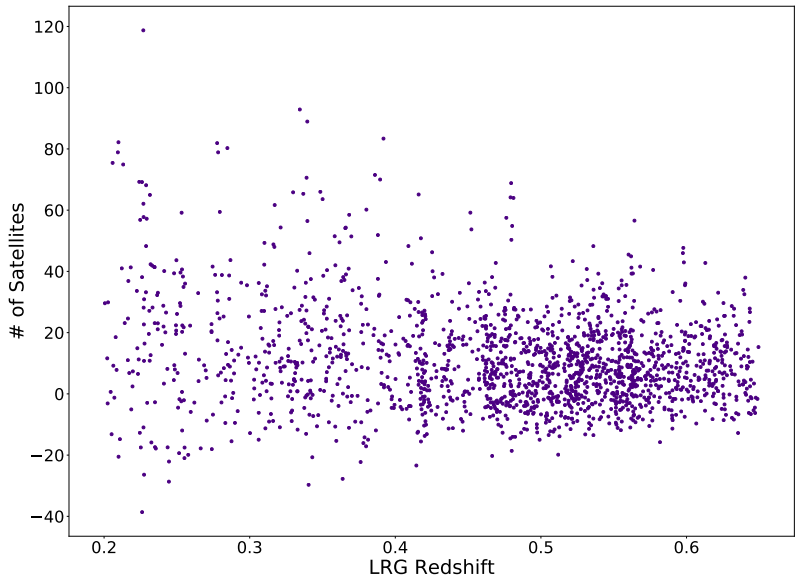

Figure 16: The number of satellites vs LRG redshift. Each point is an individual LRG in the sample. While there is a larger spread at low redshift, the number of satellites does not evolve much with redshift.

0.4.1 Caveats

The main caveat of this study is that a luminosity completeness limit has not yet been applied. This study finds statistical properties of the LRG satellite population, not the individual satellites, themselves. How to apply a luminosity cut to the satellite population is not straight-forward. A plan to implement a luminosity cut can be found in the Appendix.

0.5 Conclusions

In the hierarchical framework of galaxy evolution, we expect that small systems will form first and grow through mergers. This, however, has been difficult to test due to the lack of deep imaging over wide swath of the sky. However, thanks to the deep imaging from the Legacy Surveys, we can study relatively faint satellite galaxy properties, as well as the constraint on the importance of mergers in the formation of massie passive galaxies like LRGs. In this study we measure the

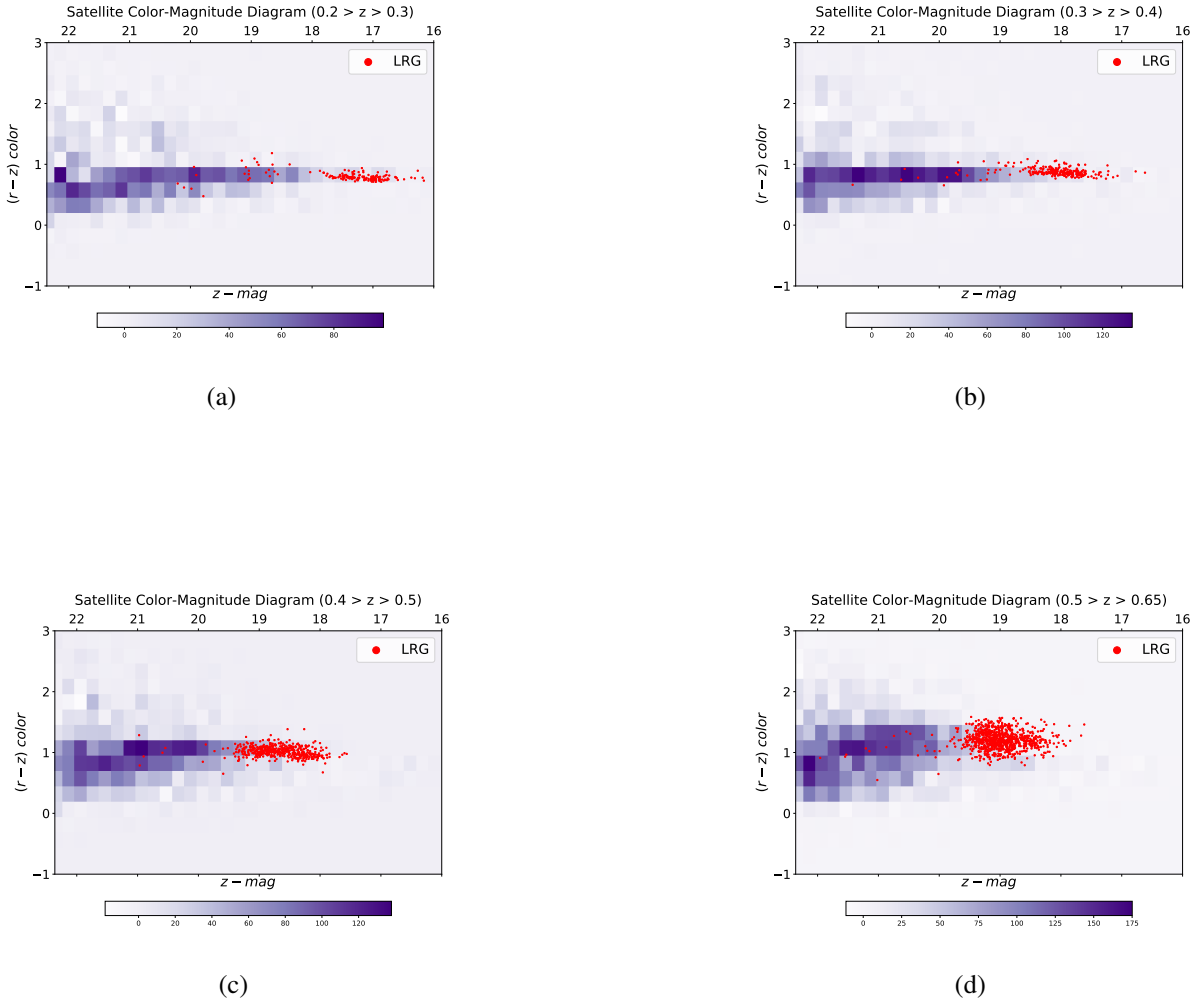

(a) (b)

(c) (d)

Figure 17: Observed color-magnitude diagram for LRGs (red dots) and satellite galaxies (shading) for different redshift bins. Each dot represents an individual LRG in this redshift range and the shaded regions represent the distribution of satellite galaxies in bins of (r-z) observed color and observed z-band magnitude. In all redshift bins the satellite population on average have bluer colors than their LRG hosts.

number and color of the satellite population of a sample of 1823 SDSS-identified Luminous Red Galaxies using Legacy Survey photometry. We use the deeper imaging of the Legacy Surveys to characterize the satellite population around LRGs as functions of LRG mass, luminosity, and redshift. This study yields three man findings:

1. The mean number of satellite galaxies over redshift range $0.2 < z < 0.65$ is 10.9 and the median is 8.6.

2. The number of satellite galaxies is not dependent on LRG redshift or mass.

3. Satellite galaxy observed colors are ore blue than observed LRG colors at all redshifts.

Since the Legacy Surveys probe about 2 magnitudes deeper than SDSS over roughly the same footprint, it provides an unprecedented opportunity to study the environments of massive elliptical galaxies.

0.6 Next Steps

In this study we have measured statistically the number and observed color of the satellite population of LRGs as functions of LRG mass, luminosity, and redshift. My next steps are to make this finding more robust by implementing a z-band luminosity cut and applying the analysis to entire Legacy Survey that overlaps with SDSS spectroscopy. I also want to find how these values change at different distances from the LRG. In this study I analyze satellites within a single search radius. I would like to quantify the statstical properties of the satellite galaxies as a funtion of distance from the LRG.

References

Banerji, M., Ferreras, I., Abdalla, F. B., Hewett, P., & Lahav, O. (2010). Exploring the luminosity evolution and stellar mass assembly of 2SLAQ luminous red galaxies between redshifts 0.4 and 0.8. *Mon. Not. R. Astron. Soc.*, 402(4), 2264–2278.

Bell, E. F., Wolf, C., Meisenheimer, K., Rix, H., Borch, A., Dye, S., Kleinheinrich, M., Wisotzki, L., & McIntosh, D. H. (2004). Nearly 5000 Distant Early-Type Galaxies in COMBO-17: A Red Sequence and Its Evolution since z 1 . *Astrophys. J.*, 608(2), 752–767.

Brammer, G. B., van Dokkum, P. G., & Coppi, P. (2008). EAZY: A Fast, Public Photometric Redshift Code. *Astrophys. J.*, 686(2), 1503–1513.

Brown, M. J. I., Dey, A., Jannuzi, B. T., Brand, K., Benson, A. J., Brodwin, M., Croton, D. J., & Eisenhardt, P. R. (2007). The Evolving Luminosity Function of Red Galaxies. *Astrophys. J.*, 654(2), 858–877.

Cool, R. J., Eisenstein, D. J., Fan, X., Fukugita, M., Jiang, L., Maraston, C., Meiksin, A., Schneider, D. P., & Wake, D. A. (2008). Luminosity Function Constraints on the Evolution of Massive Red Galaxies since z 0.9 . *Astrophys. J.*, 682(2), 919–936.

De Lucia, G. & Blaizot, J. (2007). The hierarchical formation of the brightest cluster galaxies. *Mon. Not. R. Astron. Soc.*, 375(1), 2–4.

De Lucia, G., Weinmann, S., Poggianti, B. M., Aragón-Salamanca, A., & Zaritsky, D. (2012). The environmental history of group and cluster galaxies in a Λ cold dark matter universe. *Mon. Not. R. Astron. Soc.*, 423(2), 1277–1292.

De Propris, R., Driver, S. P., Colless, M., Drinkwater, M. J., Loveday, J., Ross, N., Bland-Hawthorn, J., York, D. G., & Pimbblet, K. (2010). An upper limit to the dry merger rate at z 0.55. *Astron. J.*, 139(2), 794–802.

Dey, A., Schlegel, D. J., Lang, D., Blum, R., Burleigh, K., Fan, X., Findlay, J. R., Finkbeiner, D., Herrera, D., Juneau, S., Landriau, M., Levi, M., McGreer, I., Meisner, A., Myers, A. D., Moustakas, J., Nugent, P., Patej, A., Schlafly, E. F., Walker, A. R., Valdes, F., Weaver, B. A., Yeche, C., Zou, H., Zhou, X., Abareshi, B., Abbott, T. M. C., Abolfathi, B., Aguilera, C., Allen, L., Alvarez, A., Annis, J., Aubert, M., Bell, E. F., BenZvi, S. Y., Bielby, R. M., Bolton, A. S., Briceno, C., Buckley-Geer, E. J., Butler, K., Calamida, A., Carlberg, R. G., Carter, P., Casas, R., Castander, F. J., Choi, Y., Comparat, J., Cukanovaite, E., Delubac, T., DeVries, K., Dey, S., Dhungana, G., Dickinson, M., Ding, Z., Donaldson, J. B., Duan, Y., Duckworth, C. J., Eftekharzadeh, S., Eisenstein, D. J., Etourneau, T., Fagrelius, P. A., Farihi, J., Fitzpatrick, M., Font-Ribera, A., Fulmer, L., Gansicke, B. T., Gaztanaga, E., George, K., Gerdes, D. W., Gontcho, S. G. A., Green, G., Guy, J., Harmer, D., Hernandez, M., Honscheid, K., Lijuan, Huang, James, D., Jannuzi, B. T., Jiang, L., Joyce, R., Karcher, A., Karkar, S., Kehoe, R., Kneib, J.-P., Kueter-Young, A., Lan, T.-W., Lauer, T., Guillou, L. L., van Suu, A. L., Lee, J. H., Lesser, M., Li, T. S., Mann, J. L., Marshall, B., Martínez-Vázquez, C. E., Martini, P., des Bourboux, H. d. M., McManus, S., Menard, B., Metcalfe, N., Muñoz-Gutiérrez, A., Najita, J., Napier, K., Narayan, G., Newman, J. A., Nie, J., Nord, B., Norman, D. J., Olsen, K. A. G., Paat, A., Palanque-Delabrouille, N., Peng, X., Poppett, C. L., Poremba, M. R., Prakash, A., Rabinowitz, D., Raichoor, A., Rezaie, M., Robertson, A. N., Roe, N. A., Ross, A. J., Ross, N. P., Rudnick, G., Safonova, S., Saha, A., Sanchez, F. J., Schweiker, H., Scott, A., Seo, H.-J., Shan, H., Silva, D. R., Soto, C., Sprayberry, D., Staten, R., Stillman, C. M., Stupak, R. J., Summers, D. L., Tie, S. S., Tirado, H., Vargas-Magana, M., Vivas, A. K., Wechsler, R. H., Williams, D., Yang, J., Yang, Q., Yapici, T., Zaritsky, D., Zenteno, A., Zhang, K., Zhang, T., Zhou, R., & Zhou, Z. (2018). Overview of the DESI Legacy Imaging Surveys.

Eisenstein, D. J., Annis, J., Gunn, J. E., Szalay, A. S., Connolly, A. J., Nichol, R. C., Bahcall, N. A., Bernardi, M., Burles, S., Castander, F. J., Fukugita, M., Hogg, D. W., Ivezić, Ž., Knapp, G. R., Lupton, R. H., Narayanan, V., Postman, M., Reichart, D. E., Richmond, M., Schneider, D. P., Schlegel, D. J., Strauss, M. A., SubbaRao, M., Tucker, D. L., vanden Berk, D., Vogeley, M. S., Weinberg, D. H., & Yanny, B. (2001). Spectroscopic Target Selection for the Sloan Digital Sky Survey: The Luminous Red Galaxy Sample. *Astron. J.*, 122(5), 2267–2280.

Faber, S. M., Willmer, C. N. A., Wolf, C., Koo, D. C., Weiner, B. J., Newman, J. A., Im, M., Coil, A. L., Conroy, C., Cooper, M. C., Davis, M., Finkbeiner, D. P., Gerke, B. F., Gebhardt, K., Groth, E. J., Guhathakurta, P., Harker, J., Kaiser, N., Kassin, S., Kleinheinrich, M., Konidaris, N. P., Kron, R. G., Lin, L., Luppino, G., Madgwick, D. S., Meisenheimer, K., Noeske, K. G., Phillips, A. C., Sarajedini, V. L., Schiavon, R. P., Simard, L., Szalay, A. S., Vogt, N. P., & Yan, R. (2007). Galaxy Luminosity Functions to z˜1 from DEEP2 and COMBO-17: Implications for Red Galaxy Formation. *Astrophys. J.*, 665, 265.

Gorski, K. M., Hivon, E., Banday, A. J., Wandelt, B. D., Hansen, F. K., Reinecke, M., & Bartelmann, M. (2005). HEALPix: A Framework for High-Resolution Discretization and Fast Analysis of Data Distributed on the Sphere. *Astrophys. J.*, 622(2), 759–771.

Moustakas, J., Coil, A. L., Aird, J., Blanton, M. R., Cool, R. J., Eisenstein, D. J., Mendez, A. J., Wong, K. C., Zhu, G., & Arnouts, S. (2013). Primus: Constraints on star formation quenching and galaxy merging, and the evolution of the stellar mass function from z = 0-1. *Astrophys. J.*, 767(1).

Muzzin, A., Marchesini, D., Stefanon, M., Franx, M., Milvang-jensen, B., Dunlop, J. S., Fynbo, J. P. U., Brammer, G., & Dokkum, P. v. (2013). A public k. (pp. 1–20).

Reid, B., Ho, S., Padmanabhan, N., Percival, W. J., Tinker, J., Tojeiro, R., White, M., Eisenstein, D. J., Maraston, C., Ross, A. J., Sánchez, A. G., Schlegel, D., Sheldon, E., Strauss, M. A., Thomas, D., Wake, D., Beutler, F., Bizyaev, D., Bolton, A. S., Brownstein, J. R., Chuang, C. H.,

Dawson, K., Harding, P., Kitaura, F. S., Leauthaud, A., Masters, K., McBride, C. K., More, S., Olmstead, M. D., Oravetz, D., Nuza, S. E., Pan, K., Parejko, J., Pforr, J., Prada, F., Rodríguez-Torres, S., Salazar-Albornoz, S., Samushia, L., Schneider, D. P., Scóccola, C. G., Simmons, A., & Vargas-Magana, M. (2016). SDSS-III Baryon Oscillation Spectroscopic Survey Data Release 12: Galaxy target selection and large-scale structure catalogues. *Mon. Not. R. Astron. Soc.*, 455(2), 1553–1573.

Springel, V., Di Matteo, T., & Hernquist, L. (2005). BLACK HOLES IN GALAXY MERGERS: THE FORMATION OF RED ELLIPTICAL GALAXIES Volker Springel, 1 Tiziana Di Matteo, 1 and Lars Hernquist 2. *Astrophys. J.*, 620, L79–82.

Tojeiro, R. & Percival, W. J. (2011). Disentangling star formation and merger growth in the evolution of luminous red galaxies. *Mon. Not. R. Astron. Soc.*, 417(2), 1114–1122.

Tojeiro, R., Percival, W. J., Heavens, A. F., & Jimenez, R. (2011). The stellar evolution of luminous red galaxies, and its dependence on colour, redshift, luminosity and modelling. *Mon. Not. R. Astron. Soc.*, 413(1), 434–460.

van Dokkum, P. G., Whitaker, K. E., Brammer, G., Franx, M., Kriek, M., Labbé, I., Marchesini, D., Quadri, R., Bezanson, R., Illingworth, G. D., Muzzin, A., Rudnick, G., Tal, T., & Wake, D. (2010). The growth of massive galaxies since z = 2. *Astrophys. J.*, 709(2), 1018–1041.

Varoquaux, G., Buitinck, L., Louppe, G., Grisel, O., Pedregosa, F., & Mueller, A. (2015). Scikit-learn. *GetMobile Mob. Comput. Commun.*, 19(1), 29–33.

Appendix A

Applying Luminosity Completeness Limit to Statellite Galaxies in the Legacy Surveys

The Legacy Surveys are an observed z-band selected catalog that provides observed photometry in the g-, r-, and z-bands, as well as WISE. However, running a code like EAZY to find rest frame magnitudes in these bands is computationally expensive. To get around this problem, we use the UltraVISTA catalog to determine a rest frame z-band luminosity limit which has a 90 percent completeness limit at our redshift and observed z-band magnitude limit. The completeness limit is $\log_{10}(L/L_{\odot}) = 10.5$. The benefit of using UltraVISTA is that it is a relatively deep survey with very good photometric redshifts.

To apply this limit to Legacy Survey galaxies, we create masks based on the median luminosity of UltraVISTA galaxies in the same bin of observed (r-z) color, (g-r) color, and z-band magnitude as Legacy Survey sources using Legacy Survey photometry. We first match the UltraVISTA catlog with the Legacy Survey catalog so only UltraVISTA sources with Legacy Survey photometry are used. Then we divide the UltraVISTA sources in redshift slices of 0.02 between $0.2 < z < 0.65$, bin the sources in bins of color and magnitude, find the median rest frame z-band luminosity in that bin, and label the bin as either a 1 or a 0 if the bin has a median luminosity at or above our luminosity limit or below the luminosity limit, respectively. The rest frame z-band luminosity was found by running EAZY on the UltraVISTA sources with Legacy Survey photometry. Ultimately, for each redshift slice we have an array with the same dimensions as the arrays on which we do our statistical background subtraction. We multiply each satellite galaxy array by the mask at the appropriate redshift. This eliminates sources from color-color-magnitude bins that have a median

rest frame z-band luminosity less than $\log_{10}(L/L\odot) < 10.5$.

UltraVISTA overlaps with the southern region of the Legacy Survey, which corresponds to DECaLS. Color transformations described in Dey et al. (2018) must be used to compare DECaLS photometry to photometry from BASS and MzLS. To make appropriate luminosity limit masks for the norther region of the Legacy Surveys, we must transform the photometry and repeat the process described above. This is future work.